PHYSICAL REVIEW B **73**, 075210 (2006)

Large magnetic moments and anomalous exchange coupling in As-doped Mn clusters

Mukul Kabir,[1] D. G. Kanhere,[2] and Abhijit Mookerjee[1]
[1]*S.N. Bose National Center for Basic Sciences, JD Block, Sector III, Salt Lake City, Kolkata 700 098, India*
[2]*Department of Physics and Center for Modeling and Simulation, University of Pune, Pune - 411 007, India*
(Received 21 February 2005; published 22 February 2006)

We report electronic and magnetic properties of pure and arsenic-doped manganese clusters from density functional theory using spin-polarized generalized gradient approximation for the exchange-correlation energy. We see for both the cases, noncollinear treatment of spins are indeed necessary. The arsenic atom stabilizes manganese clusters, which is further accompanied by the ferromagnetic Mn-Mn coupling for Mn_2As and Mn_4As clusters, resulting in large cluster magnetic moments, 9 and 17 μ_B, respectively. We show in doped clusters, exchange coupling are anomalous and behave quite differently from the Ruderman-Kittel-Kasuya-Yosida-type predictions. Finally, it is suggested that, if grown in the low temperature MBE, the giant magnetic moments due to ferromagnetic Mn ordering and their large enough exchange coupling parameter in Mn_2As and Mn_4As could play an important role on the ferromagnetism and on the observed large variation in the Curie temperature of the Mn-doped III-V semiconductors.

DOI: 10.1103/PhysRevB.73.075210 PACS number(s): 75.50.Pp, 36.40.Cg, 61.46.-w

I. INTRODUCTION

Emergence of finite magnetic moment (MM) $\sim 1\mu_B$/atom in manganese clusters (Mn_{5-99}) that is antiferromagnetic as bulk (α-Mn), has been demonstrated through Stern-Gerlach (SG) deflection measurement[1] and it is readily understood to derive from the reduced atomic coordination resulting in strong *d*-electron localization. It is particularly interesting to see, what happens to the electronic and magnetic properties if we dope a single As atom to an existing Mn_x cluster to form Mn_xAs. The Mn *clustering* in ferromagnetic $Ga_{1-x}Mn_xAs$ and $In_{1-x}Mn_xAs$ samples has attracted considerable attention. The real dilute magnetic semiconductor alloys may exhibit some clustering which comes from the attractive interaction between magnetic ions[2] and, indeed, there are experimental evidences for a tendency to cluster formation.[3–5] Generally, the Mn dopant substitutes the Ga site and serves dual roles—provides local MM and acts as acceptor providing itinerant holes, which mediate ferromagnetic order. However, in reality, low substrate temperatures ($\sim$ 200–300 °C) and strong segregation tendency (of magnetic ions into semiconductor host) leads to high defect concentrations, the most important being Mn interstitials, Mn_I,[6] which are double donors that compensates holes provided by substitutional Mn_{Ga}. The increase of T_C might, therefore, related to a removal of these Mn_I defects. Different kinds of defects have been considered: Clustering[2,7,8] and random distribution[8,9] of Mn as well as Mn_I[10] and As antisites[11–13] and there is an increasing consensus that ordering increases T_c, while it decreases with clustering.[8] In recent years, Curie temperature T_c in the $Ga_{1-x}Mn_xAs$ has risen steadily, reaching $\sim$170 K for $x \sim 0.08$, when grown in layered structure and annealed at low temperature.[14–16] However, local spin-density approximation with mean-field predicts a rather high T_c for $Ga_{1-x}Mn_xAs$ (typically 350–400 K for $x \sim 0.08$).[2,17–21] This large discrepancy with experiment is attributed to uncontrolled approximations in treating the effective Heisenberg model describing interactions between localized magnetic impurities.[9,22,23] However, recently predicted T_c, assuming disorder[23,24] and percolation[9] effect, are in good agreement with the experiment.

In this paper, we address the possibility of Mn clustering around As and the consequent nature of Mn-Mn magnetic coupling? We have, indeed, found that the binding energy of Mn_xAs clusters are substantially enhanced by single As doping by having their hybridized $s-d$ electrons bond with *p* electrons of As. This *stabilization* is also accompanied by the *ferromagnetic* of Mn-Mn coupling for Mn_2As and Mn_4As clusters. Finally, we show that the exchange interactions *Js* are anomalous and behave quite differently from Ruderman-Kittel-Kasuya-Yosida (RKKY)-type theory.

II. COMPUTATIONAL METHOD

Calculations have been carried out using density functional theory, and we employed the projector augmented-wave method[25] and Perdew-Burke-Ernzerhof exchange-correlation functional[26] for the spin-polarized generalized gradient approximation, as implemented in the VASP package.[27] The wave functions are expanded in a plane wave basis set with the kinetic energy cutoff 337.3 eV and calculations have been performed at the Γ-point only. The 3*d*, 4*s* for Mn and 4*s*, 4*p* orbitals for As were treated as valence states. Symmetry unrestricted geometry optimizations were performed using quasi-Newtonian and conjugate gradient methods until all the force components are less than 0.005 eV/Å. Simple cubic supercells are used with neighboring clusters separated by at least 12 Å vacuum regions. Both collinear (CL) and noncollinear (NCL) magnetic structures have separately been considered. Several initial structures were studied to ensure that the globally optimized geometry does not correspond to the local minima, as well as we explicitly considered all possible spin multiplicities for CL case.

III. RESULTS

A. Pure Mn_n($n \leq 10$) clusters

We begin our discussion with pure Mn_x($x \leq 10$) clusters. Small clusters up to $x=4$ show ferromagnetic (FM) coupling with MM 5 μ_B/atom, the Hund's rule value for the free atom. Emergence of ferrimagnetic coupling takes place at $x=5$ and continues. Several different magnetic states lie close in energy to the ground state (GS). For an example, for trimer, the frustrated antiferromagnetic (AFM) solution is nearly degenerate (only 0.05 eV higher) with the FM solution. Small clusters prefer CL magnetic structure in their GS, whereas larger clusters adopt noncollinearity (Table I). Because of the half-filled $3d$ and filled $4s$ shell and due to the high $3d^5 4s^2 \rightarrow 3d^6 4s^1$ promotion energy, Mn atoms do not interact much as they bring together and as a result FM Mn_2 dimer is a weakly bound van der Waals (vdW) dimer with very small binding energy (BE) 0.53 eV/atom, which is evident from the low experimental value.[28] Due to the increase in the coordination number, BE increases monotonically with size x. However, this increase is not much (reaches a value 1.94 eV/atom for Mn_{10},which is 66% of the bulk value) and remain the lowest among all the $3d$ transition metal clusters.

B. Mn_nAs($n=1-10$) clusters

In the Fig. 1, we depict the GS geometries of Mn_xAs($x=1-10$) clusters with their spin ordering. The MnAs dimer has much higher BE of 1.12 eV/atom and much shorter bond length (2.21 Å) than those of Mn_2 vdW dimer. We have repeated our calculations of MnAs dimer including the Mn $3p$ as valence electrons and obtained an optimized bond length of 2.22 Å and BE of 1.08 eV/atom, with the same total MM. The BE increases substantially to 1.63 eV/atom for isosceles triangular Mn_2As, where the Mn-Mn distance ($d_{\text{Mn-Mn}}$), 2.59 Å, is almost equal to the $d_{\text{Mn-Mn}}$ in Mn_2 dimer (2.58 Å). As more Mn atoms are added, the GS structures take three-dimensional shape, and the determination of the GS become a delicate task, as several geometric and/or magnetic isomers, which are very close in energy to the GS are found and will be presented elsewhere in detail.[29] Single As-doping does not give rise to any considerable structural change, but only a moderate perturbation to the pure clusters. Usually, as x in the Mn_xAs increases BE increases due to the increase in coordination number. However, this increase is very slow after $x=2$, and tend to saturate [Fig. 2(a)]. The shortest $d_{\text{Mn-As}}$ increases from 2.21 Å for MnAs to 2.46 Å for $Mn_{10}As$, which is 4% and 2% shorter than that of in α-MnAs and $Ga_{1-x}Mn_xAs$, respectively, whereas, the shortest $d_{\text{Mn-Mn}}$ decreases: 2.56 Å for Mn_2As and 2.23 Å for $Mn_{10}As$.

TABLE I. Nature (CL/NCL) of local MM arrangement and total cluster MM (M_{tot} in μ_B) of pure Mn_x and Mn_xAs clusters, corresponding to their GS, for cluster size $x \leq 10$.

	Mn_x		Mn_xAs			Mn_x		Mn_xAs	
x	Nature	M_{tot}	Nature	M_{tot}	x	Nature	M_{tot}	Nature	M_{tot}
1	—	5	CL	4	6	NCL	12.82	NCL	1.28
2	CL	10	CL	9	7	CL	5	CL	6
3	CL	15	CL	4	8	NCL	6.83	CL	3
4	CL	20	CL	17	9	NCL	5.33	NCL	0.10
5	CL	3	CL	2	10	NCL	5.04	NCL	3.07

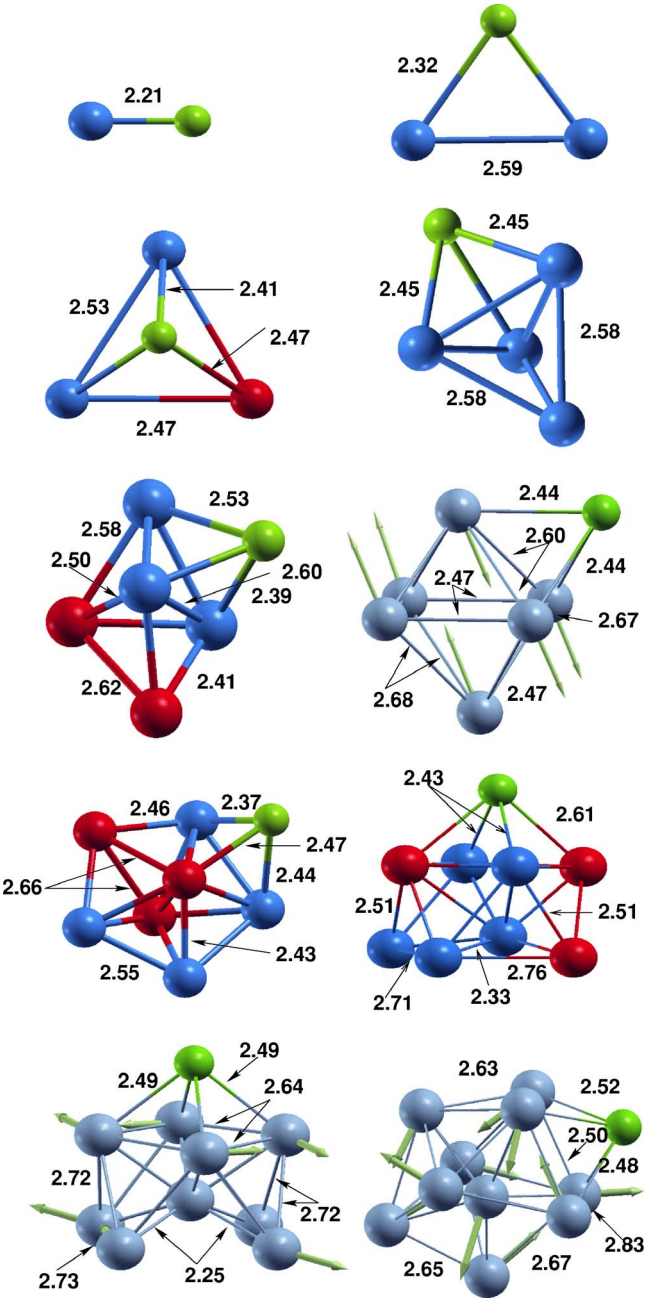

FIG. 1. (Color online) Ground state geometries and the corresponding spin ordering of Mn_xAs clusters, $x=1-10$. Atomic spin arrangements for $x=1-5,7$, and 8 are found to be collinear, where, blue and red balls represent $Mn_\uparrow$ and $Mn_\downarrow$ atoms, respectively. Whereas, they are arranged noncollinearly in $x=6,9$, and 10. Arrows are the directions of the local magnetic moments and are drawn according to their magnitudes. Green ball represents the As atom. Numbers represent the bond lengths and are given in Å. Note, only for Mn_2As and Mn_4As clusters, Mn-Mn coupling is both CL and ferromagnetic.

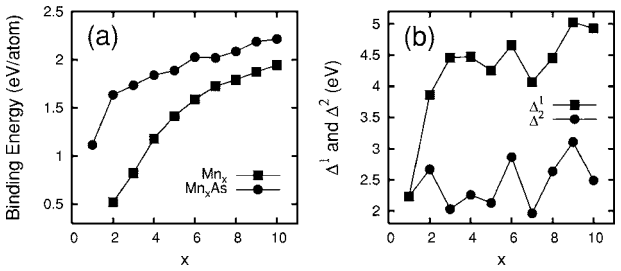

FIG. 2. (a) Plot of binding energy/atom with x, for Mn_x and Mn_xAs. (b) Two energy gains, Δ^1 and Δ^2, are plotted with x. These energy gains are defined as, $\Delta^1=-[E(Mn_xAs)-E(Mn_x)-E(As)]$ and $\Delta^2=-[E(Mn_xAs)-E(Mn_{1-x}As)-E(Mn)]$. Notice that for all x, the energy gain in adding an As-atom is larger than that of adding an Mn-atom to an existing pure Mn-cluster, i.e., $\Delta^1 \gg \Delta^2$.

The next important issue is to see whether these Mn clustering around single As are at all energetically favorable or not. To understand this point, we calculate two different energy gains, Δ^1—the energy gain in adding an As atom to a Mn_x cluster and Δ^2—the energy gain in adding a Mn atom to a $Mn_{1-x}As$ cluster. Figure 2(a) shows that due to the lack of hybridization between the $4s$ and the $3d$ electrons binding energy of pure Mn_x clusters are very small. However, as an As atom is attached, the $4s^2$ electrons of Mn interact with the $4p^3$ electrons of As, which results in the substantial enhancement in the bonding [Fig. 2(a)], and consequently, Δ^1 increases with x, which finally tends to saturate [Fig. 2(b)]. Δ^2 gives the number that how many Mn atoms can be bonded to a single As atom, which is still significant, 2.65 eV, for $Mn_{10}As$. These behaviors of $\Delta^1$and Δ^2 and more precisely, $\Delta^1 \gg \Delta^2$ for all x, indicate that the Mn clusters around As are energetically favorable and we, therefore, argue that they are, likely to be, present in the low temperature molecular beam epitaxy (MBE) grown (GaMn)As/(InMn)As.

The next obvious question is what happens to the nature of Mn-Mn magnetic coupling in these Mn_xAs clusters due to single As-doping? The total MM of Mn_xAs clusters corresponding to the respective GS geometries are given in the Table I. These large MMs, generally, arise from the ferrimagnetic coupling between the moments at the Mn-sites. However, only for Mn_2As and Mn_4As clusters, Mn-Mn coupling is FM. The nature of magnetic coupling can readily be understood form the constant spin density surface plots (Fig. 3). Like pure clusters, atomic spins are arranged collinearly in small clusters, whereas the same for larger clusters are NCL (see Table I and Fig. 1). However, for a particular sized cluster, there exists several CL and/or NCL solutions close to the GS.[29] It is interesting to note that nearest Mn-As magnetic coupling is always AFM, and therefore, As-atom forces those Mn atoms to couple ferromagnetically (see Fig. 1). The magnetization density is projected onto a sphere centering each atom to calculate the local MMs $\mathcal{M}$:

$$\mathcal{M} = \int_0^R [\rho_\uparrow(\mathbf{r}) - \rho_\downarrow(\mathbf{r})] d\mathbf{r}, \tag{1}$$

where $\rho_\uparrow(\mathbf{r})(\rho_\downarrow(\mathbf{r}))$ is the up(down)-spin density at $\mathbf{r}$ and R is the radius of the sphere centering the atom. For example, for

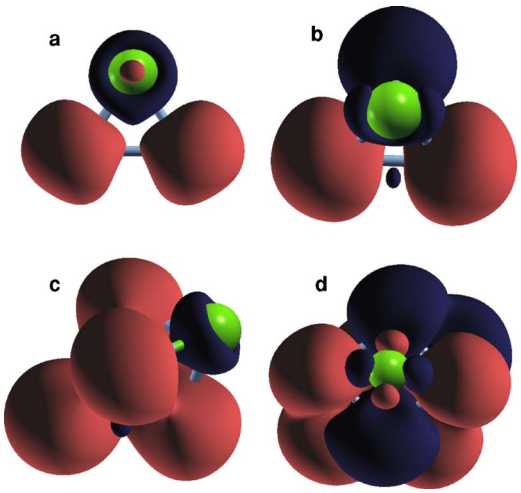

FIG. 3. (Color online) Constant spin density surfaces for Mn_2As (a), Mn_3As (b), Mn_4As (c), and Mn_8As (d) corresponding to 0.04, 0.04, 0.04, and 0.02 $e/Å^3$, respectively. All these clusters have collinear alignment in their GS. Red and blue surfaces represent positive and negative spin densities, respectively. Green ball is the As atom, which has negative polarization in all these structures. Note ferromagnetic (Mn_2As and Mn_4As) and ferrimagnetic (Mn_3As and Mn_8As) coupling between Mn atoms.

MnAs dimer, $\mathcal{M}_{Mn}$ is 3.72 μ_B and $\mathcal{M}_{As}$ is negative (−0.26 μ_B), which is very close to the negative polarization at the As-site in NiAs-type MnAs.[31] In these Mn_xAs clusters, the $\mathcal{M}_{Mn}$s are large and arise due to the strong d-electron localization at the Mn-site and the negative polarization of the anion arise from the strong $p-d$ interaction. However, $\mathcal{M}_{Mn}$s at the highly coordinated central atoms for larger clusters are very small compared to the surface atoms due to the d-electron delocalization at those sites.

IV. EXCHANGE COUPLING

To further investigate the magnetic coupling behaviour we calculate exchange interactions J_{ij}'s for the GS geometry, the magnetic energy is mapped onto a Heisenberg form:

$$\mathcal{H} = -\sum_{i,j} J_{ij} \mathbf{S}_i \cdot \mathbf{S}_j,$$

where $\mathbf{S}$ are localized magnetic moments at Mn-sites. Now we can calculate J_{ij} by computing the total energy for judicious choice of spin configurations with inequivalent combinations of pair correlation functions $\mathbf{S}_i \cdot \mathbf{S}_j$, which results in a set of linear equations for the J_{ij}'s. Calculated exchange coupling behaves anomalously to the RKKY-type predictions: J increases with the concentration as $x^{1/3}$ at 0 K and are independent of environment at fixed x. For Mn_2As cluster, exchange coupling $J(r)$ oscillates between positive and negative with $r_{Mn\text{-}Mn}$ favoring FM and AFM solutions, respectively, as well as dies down as $1/r^3_{Mn\text{-}Mn}$ [Fig. 4(a)], which is a typical RKKY-type behavior. But interestingly in contradiction with the RKKY-type predictions, we find the averaged exchange coupling $\bar{J}_{ij}$ decreases as x increases in Mn_xAs [Fig. 4(b)], however, has a very large value

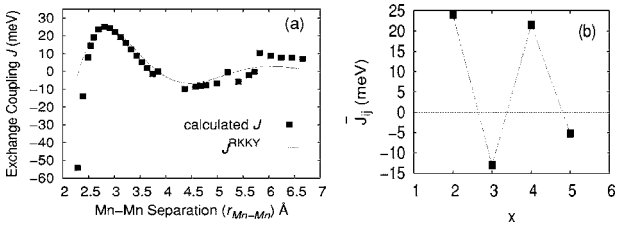

FIG. 4. (a) Dependence of exchange coupling J on the Mn -Mn spatial separation $r_{\text{Mn-Mn}}$ for Mn_2As cluster. Solid curve is the simplest RKKY form $J_{\text{RKKY}} \propto r^{-3}\cos(2k_F r)$ fitted with $k_F = 1.02$ Å^{-1}. Solid line shows excellent agreement between the calculated $J(r)$ and the RKKY model. In clusters, due to the reduced symmetry and bonding anisotropy $|\mathbf{S}_i|$ vary from site to site and, therefore, rather than the conventional $|\mathbf{S}_i| = 1$ consideration, we take $\mathbf{S}_i$ as the projected magnetization density onto a sphere of radius 1.2 Å. (b) Plot of averaged exchanged coupling $\bar{J}_{ij}$ with x for $Mn_xAs(x=2-5)$.

$\sim$21 meV for FM Mn_4As and $\bar{J}_{ij}$ has strong environment dependency.

V. SUMMARY

In summary, we have studied the electronic and magnetic properties of pure and As-doped manganese clusters, where, for both the cases, we find, the NCL treatment of atomic spins are important. FM to ferrimagnetic transition takes place at $x=5$ for pure manganese clusters. Single As-doping in the Mn_x clusters enhances the BE of resultant Mn_xAs clusters substantially. The subsequent larger energy gain in adding an As-atom to a Mn_x cluster than that of adding a Mn-atom ($\Delta^1 \gg \Delta^2$) clearly indicate the tendency of Mn "clustering" around As. The individual MM of the Mn atoms couple ferromagnetically only in Mn_2As and Mn_4As and are ferrimagnetic in nature for all other sizes studied here, whereas $Mn_xN(x \leqslant 5)$ were predicted to be all ferromagnetic.[30] However, for both pure and doped clusters, several different magnetic solutions close to the GS are possible.[29] In Mn_xAs clusters, As-atom induces FM order among its nearest neighbor Mn-atoms and calculated exchange coupling are anomalous and behave quite differently from the RKKY-type predictions. Present results can plausibly be discussed in the context of semiconductor ferromagnetism. The Mn clustering, during the low temperature molecular-beam epitaxy (MBE) growth, is energetically favorable and their presence even after annealing at a low (growth) temperature[4] could be responsible for the ferromagnetism and for the wide variation of the Curie temperature observed in the (GaMn)As samples and should be taken into account to formulate an adequate theory of ferromagnetism in the III-V semiconductors.[2] This study points out that the ferromagnetic ordering of Mn-atoms are intrinsic for Mn_2As and Mn_4As clusters and the source of effective internal magnetic field, which influences energy structure and transport. They provide the high temperature ferromagnetic contribution to the total magnetization. However, Xu and Schilfgaarde[8] recently studied the clustering effect and found that clustering decreases the Curie temperature whereas ordering increases it. But their study does not infer about any particular sized cluster. Moreover, we should note that, in dilute magnetic semiconductors the Curie temperature is controlled by the inter cluster couplings which are of long range in case of (GaMn)As.[23] The oscillatory behavior of exchange coupling J [Fig. 4(a)] will induce frustration which eventually could destabilize the ferromagnetism. The gas phase experiments involving Mn clustering in a As-seeded chamber can yield the direct information on the magnetic behavior of Mn_xAs clusters. We hope, our study will encourage such experiments.

ACKNOWLEDGMENTS

M. K. thankfully acknowledges the congenial hospitality at the Center for Modeling and Simulation of Pune University. This work has been done under the Indian Department of Science and Technology Contract No. SR/S2/CMP-25/2003.

[1] M. B. Knickelbein, Phys. Rev. Lett. **86**, 5255 (2001); Phys. Rev. B **70**, 14424 (2004).
[2] M. van Schilfgaarde and O. N. Mryasov, Phys. Rev. B **63**, 233205 (2001).
[3] J. M. Sullivan, G. I. Boishin, L. J. Whitman, A. T. Hanbicki, B. T. Jonker, and S. C. Erwin, Phys. Rev. B **68**, 235324 (2003).
[4] M. Zajac, J. Gosk, E. Grzanka, M. Kamińska, A. Twardowski, B. Strojek, T. Szyszko, and S. Podsiadlo, J. Appl. Phys. **93**, 4715 (2003).
[5] D. C. Kundaliya, S. B. Ogale, S. E. Lofland, S. Dhar, C. J. Metting, S. R. Shinde, Z. Ma, B. Varughese, K. V. Ramanujachary, L. Salamanca-Riba, and T. Venkatesan, Nat. Mater. **3**, 709 (2004).
[6] K. M. Yu, W. Walukiewicz, T. Wojtowicz, I. Kuryliszyn, X. Liu, Y. Sasaki, and J. K. Furdyna, Phys. Rev. B **65**, 201303(R) (2002).
[7] P. Mahadevan and A. Zunger, Phys. Rev. B **68**, 75202 (2003).
[8] J. L. Xu, M. van Schilfgaarde, and G. D. Samolyuk, Phys. Rev. Lett. **94**, 97201 (2005).
[9] L. Bergqvist, O. Eriksson, J. Kudrnovský, V. Drchal, P. Korzhavyi, and I. Turek, Phys. Rev. Lett. **93**, 137202 (2004).
[10] J. Blinowski and P. Kacman, Phys. Rev. B **67**, 121204(R) (2003).
[11] S. J. Postanik, K. C. Ku, S. H. Chun, J. J. Berry, N. Samarth, and P. Schiffer, Appl. Phys. Lett. **79**, 1495 (2001).
[12] S. Sanvito and N. A. Hill, Appl. Phys. Lett. **78**, 3493 (2001).
[13] P. A. Korzhavyi, I. A. Abrikosov, E. A. Smirnova, L. Bergqvist, P. Mohn, R. Mathieu, P. Svedlindh, J. Sadowski, E. I. Isaev, Yu. Kh. Vekilov, and O. Eriksson, Phys. Rev. Lett. **88**, 187202 (2002).
[14] D. Chiba, K. Tankamura, F. Matsukura, and H. Ohno, Appl. Phys.

Lett. **82**, 3020 (2003).
[15] K. W. Edmonds, P. Boguslawski, K. Y. Wang, R. P. Campion, S. N. Novikov, N. R. S. Farley, B. L. Gallagher, C. T. Foxon, M. Sawicki, T. Dietl, M. B. Nardelli, and J. Bernholc, Phys. Rev. Lett. **92**, 37201 (2004).
[16] K. C. Ku, S. J. Potashnik, R. F. Wang, S. H. Chun, P. Schiffer, N. Samarth, M. J. Seong, A. Mascarenhas, E. Johnston-Halperin, R. C. Myers, A. C. Gossard, and D. D. Awschalom, Appl. Phys. Lett. **82**, 2302 (2003).
[17] J. Kudrnovský, I. Turek, V. Drchal, F. Maca, P. Weinberger, and P. Bruno, Phys. Rev. B **69**, 115208 (2004).
[18] S. C. Erwin and C. S. Hellberg, Phys. Rev. B **68**, 245206 (2003).
[19] L. M. Sandratskii and P. Bruno, Phys. Rev. B **66**, 134435 (2002).
[20] G. Bouzerar, J. Kudrnovský, L. Bergqvist, and P. Bruno, Phys. Rev. B **68**, 081203(R) (2003).
[21] M. Sato, H. Katayama-Yoshida, and P. Dederics, Europhys. Lett. **61**, 403 (2003).
[22] K. Sato, W. Schweika, P. H. Dederichs, and H. Katayama-Yoshida, Phys. Rev. B **70**, 201202(R) (2004).
[23] G. Bouzerar, T. Ziman, and J. Kudrnovský, Europhys. Lett. **69**, 812 (2005).
[24] L. Bergqvist, O. Eriksson, J. Kudrnovský, V. Drchal, A. Bergman, L. Nordström, and I. Turek, Phys. Rev. B **72**, 195210 (2005).
[25] G. Kresse and W. Joubert, Phys. Rev. B **59**, 1758 (1999).
[26] J. P. Perdew, K. Burke, and M. Ernzerhof, Phys. Rev. Lett. **77**, 3865 (1996).
[27] G. Kresse and J. Furthmuller, Phys. Rev. B **54**, 11169 (1996).
[28] M. D. Morse, Chem. Rev. (Washington, D.C.) **86**, 1049 (1986).
[29] M. Kabir, A. Mookerjee, and D. G. Kanhere (unpublished).
[30] B. K. Rao and P. Jena, Phys. Rev. Lett. **89**, 185504 (2002).
[31] Y. Yamaguchi and H. Watanbe, J. Magn. Magn. Mater. **31-34**, 619 (1983).